

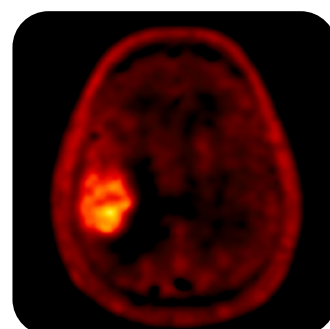
Profiles of Short Chain Fatty Acid Metabolism as Genetic Biomarkers for Primary Brain Gliomas

Marianna Inglese^[1,2], Tommaso Boccatto^[1], Matteo Ferrante^[1], Shah Islam^[2], Matthew Williams^[3,4], Adam D Waldman^[5], Kevin O'Neill^[6], Eric O Aboagye^[2], Nicola Toschi^[1,7]

[1] Department of Biomedicine and Prevention, University of Rome Tor Vergata, Italy; [2] Department of Surgery and Cancer, Imperial College London, UK; [3] Computational Oncology Group, Department of Surgery and Cancer, Imperial College London, UK; [4] Institute for Global Health Innovation, Imperial College London, UK; [5] Centre for Clinical Brain Sciences, University of Edinburgh, UK; [6] Imperial College Healthcare NHS Trust, London, UK; [7] Department of Radiology, Athinoula A. Martinos Center for Biomedical Imaging, Boston, MA, USA



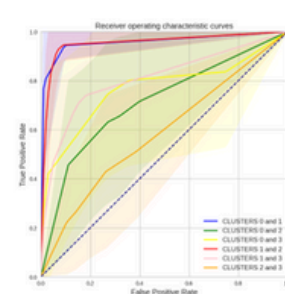
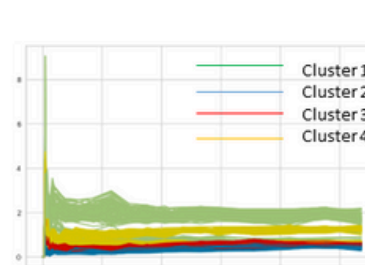
Marianna Inglese
Department of Biomedicine and Prevention
University of Rome "Tor Vergata"
marianna.inglese@uniroma2.it



INTRODUCTION

Glioblastoma multiforme (GBM) is the most common malignant primary brain tumor. The genetic profile of GBM significantly impacts its diagnosis, treatment, and patient survival. The primary biomarker for GBM is **isocitrate dehydrogenase (IDH)**. Patients with mutant IDH1/2 GBM have better outcomes compared to those with wild-type IDH tumors.^[1]

MATERIALS AND METHODS



Ten treatment-naïve patients underwent **dynamic [18F]FPIA PET/MRI**. Volumes of interest were manually drawn on the enhancing solid tumor and two reference tissues (contralateral healthy brain and superior sagittal sinus). An average of 25,202 ($\pm 14,337$) time activity curves (TACs) were extracted voxelwise from the lesion VOIs and clustered using **K-means**. A **deep model** was used to classify FPIA TACs of IDH mutant vs. wild-type GBMs, using various combinations of the clustered TACs as input.

DISCUSSION AND CONCLUSION

this study leverages the inherent spatial heterogeneity of GBMs, which significantly affects biopsy, diagnosis, and survival outcomes, to non-invasively identify four distinct spatio-temporal profiles of SCFA kinetics. These profiles are **crucial** for pinpointing particular subregions in the lesions where specific genetic mechanisms occur

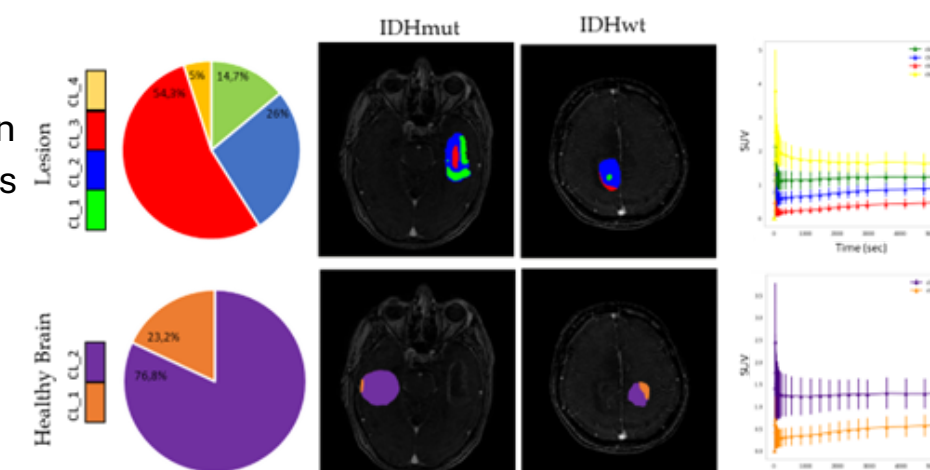
References: [1]10.2214/ajr.17.18754; [2]10.1007/s00259-012-2109-9; [3] 10.1038/s41419-020-2449-5; [4]10.1016/j.cell.2014.11.025

Acknowledgements: #NEXTGENERATIONEU (MUR); MNESYS (PNRR); MUR-PNRR M4C2I1.3 PE6 project PE00000019 Heal Italia; the NATIONAL CENTRE FORHPC, BIG DATA AND QUANTUM COMPUTING the European Innovation Council with the projects CROSSBRAIN (Grant Agreement n. 101070908) and BRAINSTORM (Grant Agreement 101099355). EOA acknowledges UK Medical Research Council award MR/N020782/1.

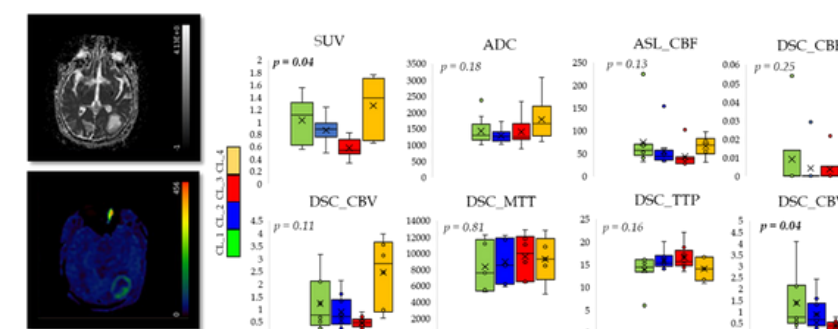
Is the distribution of short chain fatty acids (SCFA) metabolism in primary brain lesions correlated to their genetic profile (patient outcome)?

RESULTS

- K-Means algorithm found **4 different profiles of SCFA metabolism** in the lesion with a more heterogeneous distribution as compared to healthy tissues.
- SCFA metabolism described by the **combination of Clusters 1 and 2 TACs strongly represent lesion genotype** and classifies mutants from wild types with **96.15% (± 3.24) accuracy (0.96 (± 0.04) AUC)**. The worst performance was obtained by Cluster 3 with 23.67% (± 16.83) accuracy (0.31 (± 0.17) AUC), where the SUV shows the lowest values indicating deficiency of SCFA metabolism in those regions. Without considering the presence of clusters in the lesion (dFPIA) and using static PET (sFPIA) measures, the model reached lower performances.



Model	% Accuracy	AUC	Wild-Type IDH Precision	Wild-Type IDH Recall	Mutant IDH Precision	Mutant IDH Recall
Cluster 1	63.89 (± 9.55)	0.75 (± 0.13)	0.33 (± 0.32)	0.75 (± 0.41)	0.87 (± 0.23)	0.75 (± 0.14)
Cluster 2	52.70 (± 13.47)	0.59 (± 0.11)	0.59 (± 0.31)	0.79 (± 0.19)	0.71 (± 0.37)	0.39 (± 0.12)
Cluster 3	23.67 (± 16.83)	0.31 (± 0.17)	0.52 (± 0.44)	0.49 (± 0.31)	0.27 (± 0.42)	0.12 (± 0.18)
Cluster 4	63.88 (± 22.43)	0.72 (± 0.22)	0.01 (± 0.01)	0.50 (± 0.50)	0.71 (± 0.29)	0.93 (± 0.07)
Clusters 1 + 2	96.15 (± 3.24)	0.96 (± 0.04)	0.89 (± 0.10)	0.98 (± 0.04)	0.84 (± 0.31)	0.94 (± 0.06)
Clusters 1 + 3	67.82 (± 21.14)	0.71 (± 0.19)	0.74 (± 0.25)	0.76 (± 0.11)	0.50 (± 0.24)	0.67 (± 0.32)
Clusters 1 + 4	78.57 (± 27.33)	0.77 (± 0.27)	0.50 (± 0.40)	0.72 (± 0.27)	0.74 (± 0.38)	0.82 (± 0.30)
Clusters 2 + 3	62.89 (± 12.97)	0.59 (± 0.14)	0.75 (± 0.20)	0.75 (± 0.12)	0.35 (± 0.32)	0.43 (± 0.22)
Clusters 2 + 4	82.07 (± 8.35)	0.81 (± 0.09)	0.67 (± 0.27)	0.89 (± 0.06)	0.73 (± 0.35)	0.72 (± 0.14)
Clusters 3 + 4	66.37 (± 20.49)	0.58 (± 0.17)	0.78 (± 0.25)	0.81 (± 0.12)	0.44 (± 0.32)	0.35 (± 0.35)
Clusters 1 + 2 + 3	68.10 (± 14.75)	0.67 (± 0.15)	0.74 (± 0.19)	0.77 (± 0.11)	0.51 (± 0.27)	0.58 (± 0.27)
Clusters 1 + 2 + 4	83.38 (± 8.58)	0.83 (± 0.11)	0.62 (± 0.24)	0.88 (± 0.12)	0.80 (± 0.37)	0.77 (± 0.13)
Clusters 2 + 3 + 4	63.41 (± 15.14)	0.58 (± 0.13)	0.72 (± 0.17)	0.72 (± 0.15)	0.40 (± 0.29)	0.44 (± 0.25)
dFPIA	70.42 (± 16.25)	0.68 (± 0.17)	0.74 (± 0.17)	0.78 (± 0.11)	0.55 (± 0.31)	0.59 (± 0.29)
sFPIA	67.40 (± 22.87)	0.64 (± 0.16)	0.66 (± 0.22)	1.00 (± 0.00)	0.60 (± 0.49)	0.28 (± 0.33)



- Over imposing the FPIA-PET-cluster-defined subregions over the **multiparametric MRI maps** revealed subregions with a high FPIA uptake are also characterised by **restricted diffusion** (as defined by ADC maps).